TRANSPORT STUDIES OF MULTIWALLED CARBON NANOTUBES UTILIZING AFM MANIPULATION

L. ROSCHIER, J. PENTTILÄ, M. MARTIN [a], P. HAKONEN, and M. PAALANEN
Helsinki University of Technology, Low Temperature Laboratory,
P.O.Box 2200, FIN-02015 HUT, Finland

U. TAPPER and E.I. KAUPPINEN
VTT Chemical Technology, VTT Aerosol Technology Group,
P.O.Box 1401, FIN-02044 VTT, Finland

C. JOURNET [b] and P. BERNIER
Université Montpellier II,
34095 Montpellier Cedex 05, France

A multiwalled carbon nanotube (MWNT) has been manipulated into an asymmetric position between two gold electrodes on silicon dioxide surface with atomic force microscope (AFM). Transport measurements can be explained with the Coulomb staircase model assuming a semiconducting MWNT. The charging energy was found to be 24 K.

1 Introduction

Carbon nanotubes, [1] made of seamlessly wrapped graphite sheets, exhibit unique electrical and mechanical properties. There are two types of carbon nanotubes: multiwalled carbon nanotube (MWNT), where many tubes are arranged in coaxial fashion and singlewalled carbon nanotube (SWNT) consisting of only a single layer. Shortly after their discovery it was shown theoretically that the tubes are either metallic or semiconducting depending how the tubes are wrapped around. [2] Especially metallic nanotubes provide excellent building blocks for nanoelectronics and they have already been employed to demonstrate a basic SET transistor [3,4]

2 Sample preparation

The electrode structure was fabricated using electron-beam lithography on a 6×10 mm^2 substrate cut from an oxidized silicon wafer with PMMA/PMMA-MAA two-layer resist. The electrodes were 60 nm wide and consisted of 2 nm thick layer of chromium at the bottom (for adhesion) and 14 nm thick layer of gold on top. The metals were deposited using an electron-beam evaporator with a base pressure of 10^{-8} torr. The sample was cleaned in oxygen plasma before the deposition of the MWNT. A side gate was located at a distance of 500 nm.

The MWNT were synthesized with arc-discharge technique with 100 A current and 30 V voltage at 660 mbar helium atmosphere. They were purified for 45 minutes in ambient air at 750°C temperature. The tubes were dispersed in isopropanol solution and mixed ultrasonically. A droplet of this solution was deposited on the substrate and the sample was kept for 5 minutes in isopropanol atmosphere. Then the droplet was blown off with dry nitrogen gas. Figure 1 illustrates transmission electron microscope images of the MWNT taken from the same solution as the moved MWNT. The roughness and shape correspond to those reported by other groups. [5]

[a] present address: K.U. Leuven, Laboratory for Molecular Dynamics and Spectroscopy, Celestijnenlaan 200F, BE-3001 Heverlee, Belgium
[b] present address: Max-Planck-Institut für Festkörperforschung, Heisenbergstr. 1, D-70569 Stuttgart, Germany

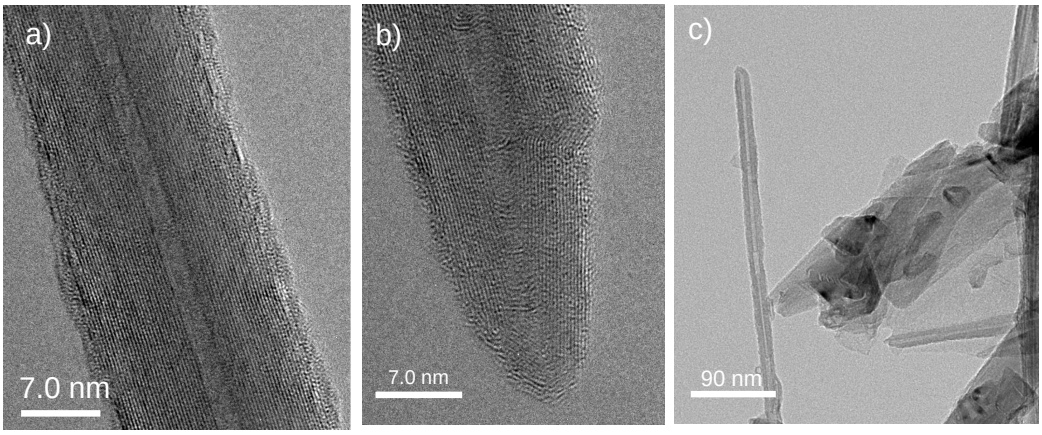

Figure 1: Transmission electron microscope images of MWNTs. a) and b) show the middle part and the end of a MWNT. c) illustrates dirt remaining even after the purification in the oven.

3 Manipulation with AFM

Since 1995 scanning probe microscopes have been used to manipulate small particles.[6] Recently, they have been employed to move MWNTs.[7] One application has been the study of friction between the substrate and the MWNT.[8]

We employed *Park Scientific Instruments* (PSI) *CP* AFM with *Ultralever* cantilevers. *ProScan* software from PSI was used to image the sample surface and to manipulate one of the tubes on top of it. The manipulation scheme was about the same as we have previously used to move 45 nm silver particles.[9] With this method AFM was operated in noncontact mode (NCM).[10] We moved a MWNT that was 410 nm long and had a diameter of 20 nm according to the AFM images, and placed it between two electrodes separated by 250 nm

The moving went as follows. First the surface was imaged in NCM. When a tube was found, the feedback-loop was cut off. Simultaneously NCM signal was monitored and tip-sample distance was decreased in small steps of some nanometers. When the tube was hardly visible in the NCM signal, the tube usually moved. Sometimes the tip dragged the tube, sometimes it pushed the tube. Thus the moving procedure was a trial and error procedure. The moving of the tube was composed of a set of rotations. The process to move the tube from a distance over 1 μm to the electrodes took around 100 pushes/images. It is notable that it was possible to lift the tube on top of the electrode which had a thickness larger than the tube radius. Figure 2 illustrates some images taken during the moving process.

4 Transport measurements

Transport measurements were done at low temperatures with a plastic dilution refrigerator. The sample resistance was tracked with 100 mV DC voltage to decrease from 5 MΩ to 9 MΩ when the sample was cooled from 300 K to 4 K. Fig. 3a illustrates the measurement configuration we used at low temperatures. We made our measurements at T=120 mK.

The measurements indicate a 15 mV wide zero current plateau across zero-voltage bias as is illustrated in Fig. 3b. Because of the asymmetry of the junctions, we presume a Coulomb staircase model,[11] where the current through the tube is determined mostly by the more resistive tunnel junction between the tube and the electrode. The shape of the $I(V_{bias})$ curve is mostly due to the density of states that have a major influence on the tunneling process. Thus, we think the peaks in Fig. 4a are traces of van Hove singularities, at which a new conduction band opens

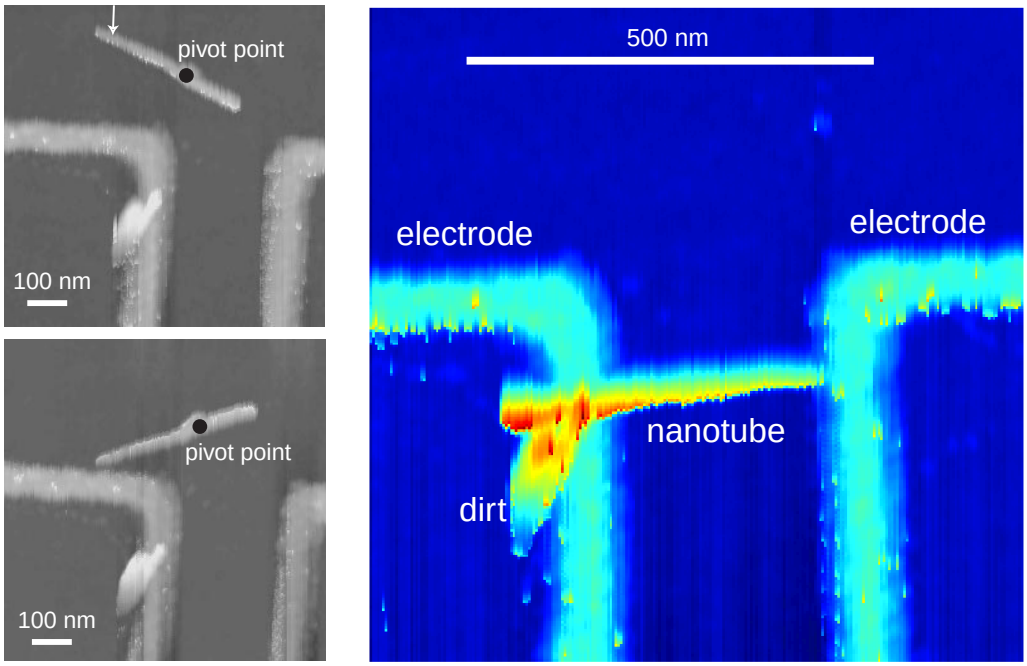

Figure 2: Two AFM images, taken during the moving process, are displayed on the left. The arrow indicates where tube was pushed. The pivot point of rotation is marked. On the right, the tube is in its final position. Note that the right end touches the electrodes lightly whereas the left one is well over the electrode.

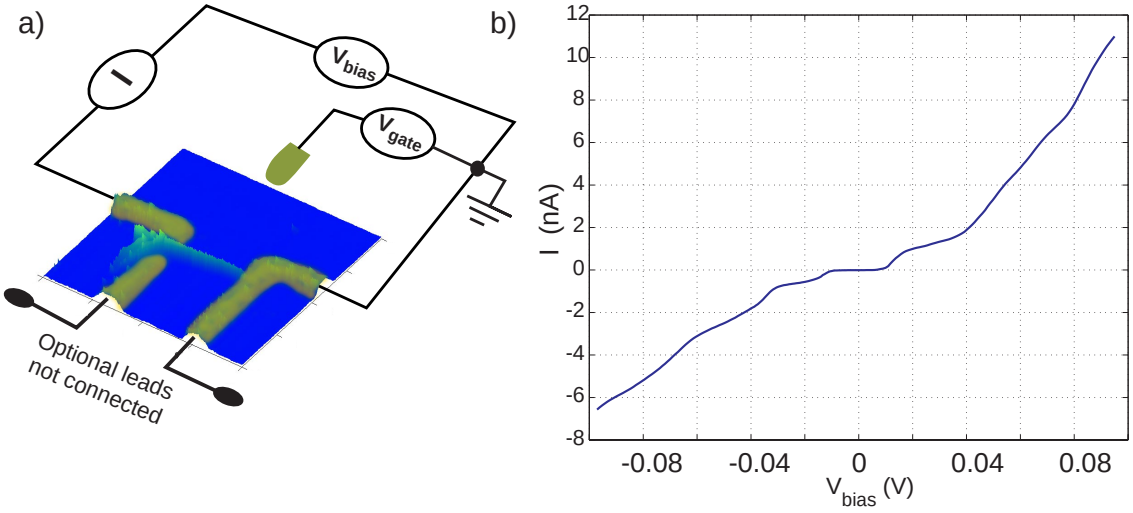

Figure 3: a) The biasing configuration. b) The measured $I(V_{bias})$ curve at 120 mK.

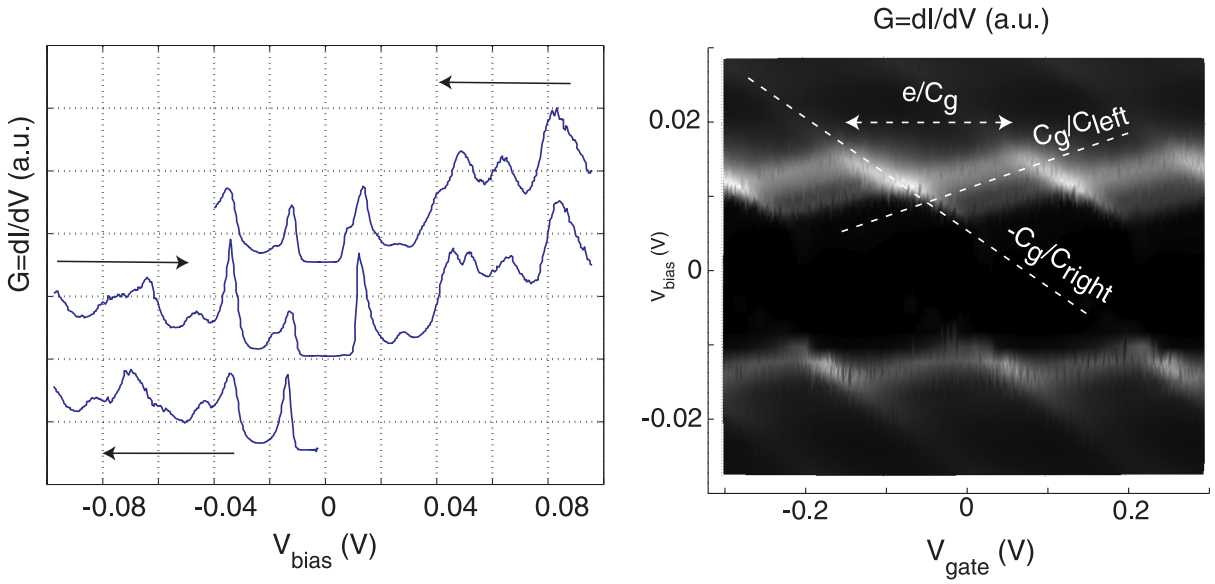

Figure 4: a) Differential conductance as a function of V_{bias}. The arrows indicate the sweep direction. At the turning points, the curves are shifted vertically. b) Averaged differential conductance $G = dI/dV_{bias}$ as a function of V_{bias} and V_{gate}. A lighter color denotes a higher conductance. The white dotted lines denote slopes that were used to extract the capacitances.

for electrons or holes. The gap addresses the MWNT to be semiconducting. We expect that the outermost layer of the MWNT determines mostly the electrical transport properties of the MWNT as is the case in graphite where the intra-layer conductance is 10^{-5} times smaller than the in-plane conductance. [12] The differential conductance is hysteretic as seen in Fig. 4, where the peak shapes are slightly different depending on the V_{bias} sweep direction. We believe the hysteresis can be attributed to charge trapping, [13] in which single electrons tunnel hysteretically across the concentric tubes.

Figure 4b illustrates differential conductance $G = dI/dV_{bias}$ as a function of V_{gate} and V_{bias}. It is constructed from a set of $G(V_{gate})$ curves with different V_{bias} values. The periodic single charging effect of the gate modulation to the differential conductance is obvious. From the modulation period we extract the value for the gate capacitance $C_g = 0.8$ aF. The gate modulation cannot make the MWNT to conduct at the zero bias voltage. The single set of parallel ridges matches the Coulomb staircase model. We relate the slopes drawn in Fig. 4b to the capacitance ratios $-C_g/C_{right}$ and C_g/C_{left} and found the values $C_{left} = 26$ aF and $C_{right} = 11$ aF. [14] In the latter value we gave more weight to the slopes of the ridges. C_{left} was determined from the conduction edge. The total capacitance yields for the charging energy $E_C = e^2/2(C_{left} + C_{right} + C_g) = 2.1$ meV.

5 Conclusions

Our transport measurements on a semiconducting MWNT between two gold electrodes exhibited clear single electron charging effects on top of a 15 mV conductance gap. The observed gap coincides with previous experiments on SWNT [15] if scaling with the tube diameter is taken into account. The Coulomb staircase model agrees well with our data on charging effects, even though the density of states on the carbon nanotube strongly influences the IV-characteristics. The capacitance and resistance of Au/nanotube junctions were obtained from SET modulation curves above the conductance gap. The method to move MWNTs with AFM combined with electron-beam 'soldering' [16] may provide new opportunities to make optimized tunnel junctions.

This may prove useful in the future 'single electron' components made with nanotubes.

Acknowledgments

The authors want to thank M. Ahlskog and E. Sonin for useful discussions. This work was supported by the Academy of Finland, by TEKES of Finland via the Nanotechnology program, and by the Human Capital and Mobility Program ULTI of the European Community.

References

1. S. Iijima, Nature (London) **354**, 56 (1991).
2. J.W. Mintmire, B. I. Dunlap, and C. T. White, Phys. Rev. Lett. **86**, 631 (1992); N. Hamada, S. Sawada, and A. Oshiyama, ibid **86**, 1579 (1992); R. Saito, M. Fujima, G. Dresselhaus, and M. S. Dresselhaus, Appl. Phys. Lett. **60**, 2204 (1992).
3. M. Bockrath, D.H. Cobden, P.L. McEuen, N. G. Chopra, A. Zettl, A. Thess, and R.E. Smalley, Science **275**, 1922 (1997).
4. S. J. Tans, M. H. Devoret, H. Dai, A. Thess, R. S. Smalley, L. J. Geerlings, and C. Dekker, Nature (London) **386**, 474 (1997); S. J. Tans, A.R.M. Verschueren, and C. Dekker, Nature (London) **393**, 49 (1998).
5. *Handbook of Microscopy, Applications in Materials Science, Solid-State Physics and Chemistry*, edited by S. Amelinckx, D. van Dyck, J. van Landuyt, and G. van Tendeloo, (VCH, Weinheim, 1997), p. 458.
6. T. Junno, K. Deppert, L. Montelius, and L. Samuelson, Appl. Phys. Lett. **66**, 3627 (1995).
7. T. Hertel, R. Martel, and P. Avouris, J. Phys. Chem. B **102**, 910 (1998).
8. M.R. Falvo, R.M. Taylor, A. Helser, V. Chi, F.P. Brooks Jr, S. Washburn, and R. Superfine, Nature (London) **397**, 236 (1999).
9. M. Martin, L. Roschier, P. Hakonen, Ü. Parts, M. Paalanen, B. Schleicher, and E. I. Kauppinen, Appl. Phys. Lett. **73**, 1505 (1998).
10. T. R. Ramachandran, C. Bauer, A. Bugacov, A. Madhukar, B. E. Koel, A. Requicha, and C. Gazen, Nanotechnology **9**, 237 (1998).
11. See, *e.g.*, A.E. Hanna and M. Tinkham, Phys. Rev. B **44**, 5919 (1991).
12. B.T. Kelly, *Physics of graphite*, (Applied Science, London, 1981), p. 294.
13. P.D. Dresselhaus, L. Ji, Siyuan Han, J.E. Lukens, and K.K. Likharev, Phys. Rev. Lett. **72**, 3226 (1994).
14. L. Roschier, J. Penttilä, M. Martin, U.Tapper, C. Journet, P. Bernier, E.I. Kauppinen, P. Hakonen, and M. Paalanen, to be published.
15. J.W.G. Wildöer, L.C. Venema, A.G. Rinzler, R.E. Smalley, and C. Dekker, Nature (London) **391**, 59 (1998).
16. A. Bachtold, M. Henny, C. Terrier, C. Strunk, C. Schönenberger, J.-P. Salvetat, J.-M. Bonard, and L. Forrò, Appl. Phys. Lett. **73**, 274 (1998).